Molecular Crystals and Liquid Crystals

Publication details, including instructions for authors and subscription information:
http://www.tandfonline.com/loi/gmcl20

Inverse Frederiks Effect and Bistability in Ferronematic Cells

V. I. Zadorozhnii [a] , V. Yu. Reshetnyak [a] , A. V. Kleshchonok [a] , T. J. Sluckin [b] & K. S. Thomas [c]

[a] Physics Faculty, Kyiv National Taras Shevchenko University, Kyiv, Ukraine

[b] Faculty of Mathematical Studies, University of Southampton, Southampton, United Kingdom

[c] School of Electronics and Computer Science, University of Southampton, Southampton, United Kingdom

Version of record first published: 22 Sep 2010

To cite this article: V. I. Zadorozhnii, V. Yu. Reshetnyak, A. V. Kleshchonok, T. J. Sluckin & K. S. Thomas (2007): Inverse Frederiks Effect and Bistability in Ferronematic Cells, Molecular Crystals and Liquid Crystals, 475:1, 221-231

To link to this article: http://dx.doi.org/10.1080/15421400701732019

Mol. Cryst. Liq. Cryst., Vol. 475, pp. 221–231, 2007

ISSN: 1542-1406 print/1563-5287 online
DOI: 10.1080/15421400701732019

Taylor & Francis
Taylor & Francis Group

Inverse Frederiks Effect and Bistability in Ferronematic Cells

V. I. Zadorozhnii
V. Yu. Reshetnyak
A. V. Kleshchonok
Physics Faculty, Kyiv National Taras Shevchenko University, Kyiv, Ukraine

T. J. Sluckin
Faculty of Mathematical Studies, University of Southampton, Southampton, United Kingdom

K. S. Thomas
School of Electronics and Computer Science, University of Southampton, Southampton, United Kingdom

In recent work we have examined switching properties of a ferronematic in an external magnetic field in a cell with homeotropic boundary conditions, and subject also to a bias field in the plane of the cell. There are three regimes, depending on the strength of the director-ferroparticle coupling. For low coupling, there is a high field inverse Frederiks transition to an undistorted phase. At low non-dimensional temperatures, high magnetic fields can cause the ferroparticles to segregate. Segregation-director distortion coupling can drive the inverse Frederiks transition first order, causing bistability. This article considers homogeneous planar, rather than homeotropic anchoring at the cell walls and particle surfaces. The bias field is unnecessary, but the basic physical picture is retained, with the same set of regimes. The lack of bias field means that this case is a more suitable model for basic studies.

Keywords: ferroparticle; liquid crystal; magnetic field

We are grateful to S. V. Burylov, I. P. Pinkevich, A. N. Vasilev and M. P. Allen for useful discussions. INTAS (grant no. 99-00312) and NATO (grant no. CBP.NUKR.CLG.981968) have supported visits to Southampton by VYR and VIZ, and a visit to Kiev by TJS. We thank these agencies for continuing support. One of the authors (AVK) acknowledges support from the Victor Pinchuk Foundation (Zavtra.UA scholarship program).

Address correspondence to T. J. Sluckin, Faculty of Mathematical Studies, University of Southampton, Southampton, SO17 1BJ, United Kingdom. E-mail: t.j.sluckin@soton.ac.uk

1. INTRODUCTION

The prediction in 1970 by Brochard and de Gennes [1] of the existence of magnetic colloids embedded in a liquid crystal matrix (so-called ferronematics (FN)) has been extremely fruitful. Early experiments [2,3] encouraged Burylov and Raikher [4] to generalize a theoretical model to the soft anchoring case. More recently Berejnov *et al.* [5] have synthesized stable lyotropic ferronematic solutions, and Buluy *et al.* [6,7] have synthesized a stable suspension of (thermotropic) 5CB. The colloidal particles are needle-like Fe_3O_4 ferroparticles, coated with oxyethyl-propylene glycol to counteract colloidal aggregation.

The key relevant properties of a nematic crystal doped with single-domain anisometric ferromagnetic particles are: (a) high intrinsic magnetic susceptibility, and (b) uniform molecular reorientation of the entire LC matrix in a varying magnetic field, a phenomenon known as macroscopic collective behavior [1]. The liquid crystal molecular orientation can then controlled by applying easily accessible magnetic fields $\sim$10 Oe. At these fields there are practical applications, for example in magnetically-controlled devices for information processing and storage.

In recent work [8], we have examined a FN system with homeotropic anchoring at cell walls and particle surfaces. The imposed magnetic field had a propensity to reorient the nematic director normal to the cell boundaries. A bias field in the plane of the cell is also required to restrict rotation of the magnetic director to one plane. Otherwise the magnetic director will be thermally disoriented, and in the low field regime, it will not be a well-defined quantity.

Now the imposed magnetic field reorients the director. But if the particle-field coupling is sufficiently weak, there is an inverse Frederiks effect at high fields, and the nematic director reverts to its initial texture. There is also a possibility of magnetic segregation: magnetic colloidal particles migrate towards regions in which the FN free energy of FN is minimized, but this is opposed by entropic forces favoring a uniform colloidal concentration. The segregation couples to the director distortion, driving the inverse Frederiks transition first order. The consequence is a possible bistable director response.

In this article we extend [8] to systems with homogeneous planar anchoring. A bias field is no longer necessary. Our calculations solve a full continuum-statistical mechanical theory, and the results are also analyzed using simplified models. The key result is that the fundamental switching properties of the FN system [8] are robust with respect to change of boundary condition from homeotropic to homogeneous planar.

2. MODEL

The geometry of the problem is shown in Figure 1.

A cell of thickness D is filled with ferronematic initially oriented parallel to the cell planes, subject to strong planar nematic anchoring at the cell walls at $z = 0$ and $z = D$. The cell is uniform in the $x - y$ direction. The anchoring energy at the ferroparticle surfaces favors weak planar anchoring. The cell is subject to an external magnetic field normal to the cell walls. The magnetic particles are needle-like monodomain ferrite grains of length L and diameter $d \sim L/7 - L/3$, significantly greater than the nematic molecule size. In the initial state ferroparticles are homogeneously distributed over the cell volume and their magnetic moments are perpendicular to the unperturbed director $\hat{\mathbf{n}}_0$. $\hat{\mathbf{m}}_0$ (unperturbed magnetic director) is the unit vector in the direction of the sample magnetization at $\mathbf{H} = 0$.

The FN equilibrium configurations at given magnetic field $\mathbf{H}$ are obtained by minimizing the free energy functional [4,9]

$$F = \int_V \left\{ \frac{1}{2} \left[K_1 (\operatorname{div} \hat{\mathbf{n}})^2 + K_2 (\hat{\mathbf{n}} \cdot \operatorname{curl} \hat{\mathbf{n}})^2 + K_3 (\hat{\mathbf{n}} \times \operatorname{curl} \hat{\mathbf{n}})^2 \right] - M_s f (\hat{\mathbf{m}} \cdot \mathbf{H}) - 2f W_p (\hat{\mathbf{n}} \cdot \hat{\mathbf{m}})^2 + \frac{f k_B T}{v} \ln f \right\} dV \tag{1}$$

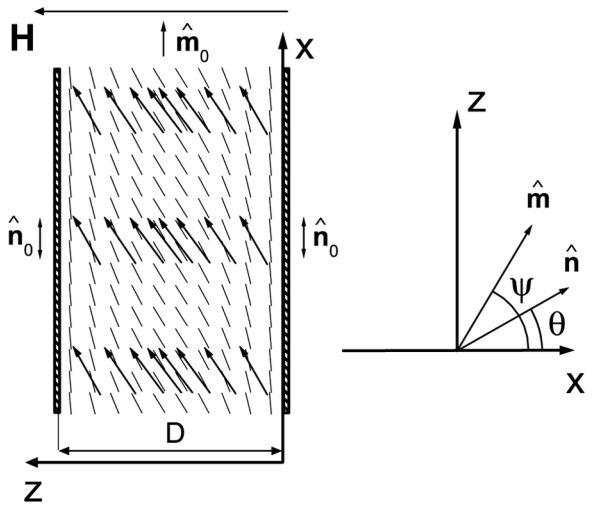

FIGURE 1 Schematic of the FN cell. The nematic and magnetic rotational distortions in an external magnetic field are given respectively by $\hat{\mathbf{n}} = [\cos\theta(z), 0, \sin\theta(z)]$, and $\hat{\mathbf{m}} = [\cos\psi(z), 0, \sin\psi(z)]$.

subject to ferroparticle number conservation

$$\int f\, dV = \bar{f} V, \tag{2}$$

where K_1, K_2, K_3 are elastic (Frank) constants, f and $\bar{f}$ are the local and the mean volume particle fractions, $\hat{\mathbf{n}}$ is a nematic director, $\hat{\mathbf{m}}$ is the unit vector in the direction of the sample magnetization, M_s is the saturation magnetization per unit volume within an individual colloidal particle, W_p is the effective soft planar anchoring energy per colloidal particle due to the nematic-ferroparticle surface interaction [4,8], and v is the colloidal particle volume. At low nematic-ferroparticle orientational coupling ($W_p v \leq k_B T$) the magnetization sometimes is reduced from this saturation value by thermal fluctuation effects [4]. We suppose here the magnetization of the ferroparticles to have reached saturation.

We also note, as compared to the homeotropic anchoring case, the absence of a bias field term. The planar homogeneous anchoring case has a number of advantages with respect to the homeotropic system. In addition to the lack of bias field, the anchoring energies far exceed those at homeotropic surfaces, resulting in an enhanced response.

The term in square brackets in Eq. (1) is the Frank-Oseen-Zocher curvature energy. The remaining terms are respectively: the magnetic energy of the colloidal particles, the anchoring-induced ferronematic interaction, and the contribution of the mixing entropy of an ideal ferroparticle solution. We neglect the ferroparticle magnetic dipole-dipole interaction energy, which disappears at low ferroparticle concentrations, and the direct magnetic-nematic interaction, which in the magnetic fields under consideration ($H < 200$ Oe) is small as compared to the indirect colloidally-mediated coupling [11].

Now we non-dimensionalize the problem, introducing the dimensionless magnetic field $h = \bar{f} M_s H D^2 / K$, the dimensionless coupling between the nematic and magnetic orientations $w = 2\bar{f} W_p D^2 / K$ (note that W_p, unlike [4], is now per unit volume), and the dimensionless temperature $t = k_B T \bar{f} D^2 / (vK)$, where K is the mean value of elastic constants. In the real problem t takes its physical value, but it is useful nevertheless to treat it as a variable parameter in the theory.

In the one-constant approximation the scaled free energy functional becomes

$$F = \int_0^1 dz \left[\frac{1}{2} \left(\frac{d\theta}{dz} \right)^2 - \eta h \sin\psi - \eta w \cos^2(\theta - \psi) + \eta t \ln \eta \right], \tag{3}$$

subject to boundary condition $\theta(0) = \theta(D) = 0$ and the constraint $\int_0^1 \eta(z)dz = 1$, where z is now measured in units of the cell width D and $\eta(z) = f(z)/\bar{f}$ is the local change of the colloidal density induced by segregation effects.

To make contact with experiment, we consider a cell of thickness $D = 250\,\mu\text{m}$, magnetic particles of $L = 0.1\,\mu\text{m}$, $d = L/3$ and use typical experimental and material parameter values $W_p d \approx 9.5 \times 10^{-3}\text{erg/cm}^2$, $\bar{f} \approx 3.6 \times 10^{-7}$, $K = 5.3 \times 10^{-7}\text{dyn}$, $M_s = 485$ G. These values are representative of a 5CB liquid crystal at $T = 25^\circ\text{C}$ and magnetite particles [7,10–12]. These considerations imply $t = 0.2$ and $w = 2.42$. With a cell thickness $D = 460$ μm, mean volume fraction $\bar{f} = 6.9 \times 10^{-6}$ and magnetic particles with $L = 0.15$ μm and $d = L/3$, we estimate $t = 3.85$.

The Euler-Lagrange equations corresponding to Eq. (3) are:

$$\frac{d^2\theta}{dz^2} - \eta w \sin(2(\theta - \psi)) = 0, \tag{4}$$

$$h \cos\psi + w \sin(2(\theta - \psi)) = 0, \tag{5}$$

$$\eta = e \Big/ \int_0^1 e dz, \tag{6}$$

where $e(\theta, \psi) = \exp\left[(h \sin\psi + w \cos^2(\theta - \psi))/t\right]$. We note that in the limit $t \to \infty$ there is no colloidal segregation and the colloidal density is elsewhere constant $\eta(z) = 1$.

The boundary conditions $\psi(0) = \psi(1) = \psi_s$ are not defined explicitly. Strong planar anchoring at the cell walls yields $\theta(0) = \theta(1) = \theta_s = 0$, and from Eq. (5) we find $h \cos\psi_s = w \sin(2\psi_s)$. This equation sustains two solutions: (a) $\psi_s = \arcsin(h/2w)$ in the low magnetic field case $(h < 2w)$ and (b) $\psi_s = \pi/2$ in the high field case $(h > 2w)$; there is a change of regime at $h = 2w$.

We can make a Landau expansion of F around $\psi = \pi/2$, $\theta = 0$ in powers of θ and $\gamma = \frac{\pi}{2} - \psi$. As in the related homeotropic FN system [8], there are three regimes, depending on the value of w. In the low coupling regime $w < w_c = \pi^2/2$ there is an inverse Frederiks effect: the nematic reorientation increases and then reduces, disappearing at a critical field $h_c(w) = 2ww_c/(w_c - w)$ (Fig. 2(a), curve 1). The critical value w_c is the field corresponding to the Frederiks transition. For $h > h_c(w)$ the magnetic particles are completely aligned with the magnetic field (Fig. 2(b), curve 1). At intermediate coupling $w_c < w < w^* \approx 3w_c/2$ the degree of reorientation reduces at high fields but remains finite. For high coupling $w > w^*$ the director switching saturates.

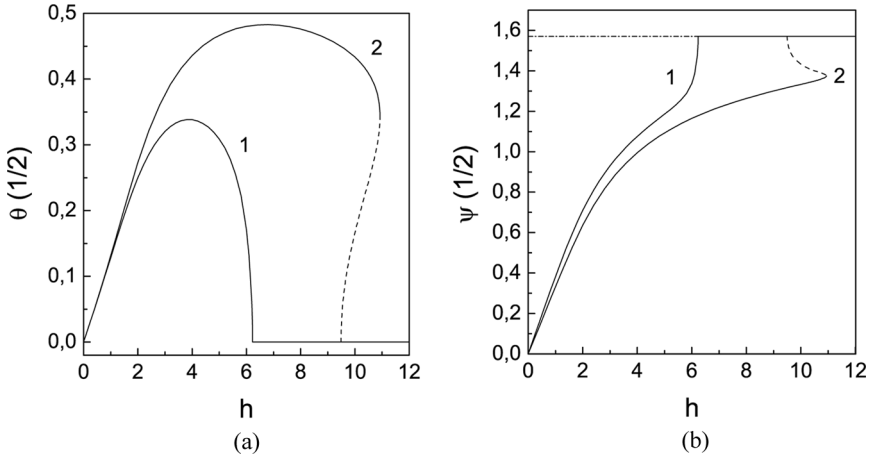

(a) (b)

FIGURE 2 Nematic (a) and magnetic (b) director distortions in the middle of the cell ($z = 1/2$) for weak ferronematic coupling at finite temperature $t = 0.2$ as a function of external field. $w = 1.91$, $t > t_c = 0.15$ (curve 1) and $w = 2.42$, $t < t_c = 0.3$ (curve 2).

3. INVERSE FREDERIKS EFFECT AND BISTABLE STATE

Now we focus on the case of the low coupling and low dimensionless temperature t when the segregation effect comes into play. Redistribution of the ferroparticles in z is opposed by entropic forces favoring a uniform colloidal concentration. The balance is controlled by t.

We analyze the properties of this model in the high field regime ($h \geq 2w$). To find the approximate expressions for the angles $\theta(z)$, $\psi(z)$ and the segregation function $\eta(z)$ we express the angular and segregation quantities in terms of a Fourier series, truncating beyond the leading terms:

$$\psi = \frac{\pi}{2} - \gamma, \quad \gamma = \gamma_0 \sin \pi z, \quad \theta = \theta_0 \sin \pi z, \quad \eta(z) = 1 - 2s \cos 2\pi z, \quad (7)$$

where $\theta_0 = \theta(1/2)$; $\gamma_0 = \pi/2 - \psi_0$, with $\psi_0 = \psi(1/2)$; the quantity s is defined by $s = -\int_0^1 dz\, \eta(z) \cos 2\pi z$. Note that the boundary conditions on θ and ψ are automatically satisfied. As $s = 0$ if the ferrocolloid is unsegregated ($\eta = 1$ everywhere), whereas $s = 1$ if perfectly segregated (ferroparticles are confined to $z = 1/2$), we can label s as the segregation order parameter. We can describe the degree of segregation using the order parameter s provided that the temperature t is high enough and η is small.

We consider a particularly interesting case of the low coupling $w < w_c$ regime. After substituting Eq. (7) into the scaled free energy functional, expanding trigonometric and logarithmic functions into power series in γ_0, θ_0 and s up to fourth order (we will see that $s \sim \gamma_0^2$) and integrating, we derive an expression for the cell free energy

$$F \sim (w_c - w)(\theta_0 - \beta_c(w)\gamma_0)^2 + \frac{(h - h_c(w))}{2}\gamma_0^2 + 2ts^2 - w(\theta_0 + \gamma_0)^2 s + \frac{h}{2}\gamma_0^2 s + \frac{w}{4}(\theta_0 + \gamma_0)^4 - \frac{h}{32}\gamma_0^4, \tag{8}$$

where $\beta_c(w) = h_c(w)/(2w_c)$. At $h > h_c(w)$ there is no structure at all, for now $\psi(z) = \pi/2$ and $\theta(z) = 0$. In this regime $s = 0$ and there is no segregation. For $h < h_c(w)$ the first term is positive, the second is negative and we should make a Landau expansion $\theta_0 = \beta_c(w)\gamma_0 + \cdots$. After inserting θ_0 into Eq. (8) and minimizing the functional, we find that just below the inverse Frederiks transition

$$\gamma_0 = \left(\frac{w_c}{w} - 1\right)\theta_0. \tag{9}$$

For s and γ_0 we find equations

$$s = \frac{h_c(w)}{16t}\left[\frac{h_c(w)}{w_c} + 2\left(1 - \frac{h}{h_c(w)}\right)\right]\gamma_0^2, \tag{10}$$

$$\gamma_0^2 = 8\frac{\frac{sh_c(w)}{w_c} + 2(1+s)\left(1 - \frac{h}{h_c(w)}\right)}{\left(\frac{h_c(w)}{w}\right)^3 - 2\frac{h}{h_c(w)}}. \tag{11}$$

Thus, there is structure in $\psi(z)$, $\theta(z)$ and so $\eta(h) \neq 0$ for $h < h_c(w)$ (see Fig. 3). As a result the order parameters s and γ_0 couple in a Landau expansion of the free energy of the system close to $h_c(w)$. The coupling is constant, but the stabilizing term in s is proportional to t. It is this fact which gives rise to the general result $s \sim t^{-1}$.

After substituting Eqs. (9)–(11) into (8), we find at $h = h_c(w)$

$$F \sim \frac{h_c(w)}{32}\left[\frac{h_c^3(w)}{2}\left(\frac{1}{w^3} - \frac{1}{2t\,w_c^2}\right) - 1\right]\gamma_0^4. \tag{12}$$

The existence of a coupled order parameter can drive a previously continuous transition first order [13]. Close to $h = h_c(w)$ the coupling of the order parameters reduces and eventually changes the sign of the γ_0^4 term in the Landau expansion. A negative γ_0^4 term signals that

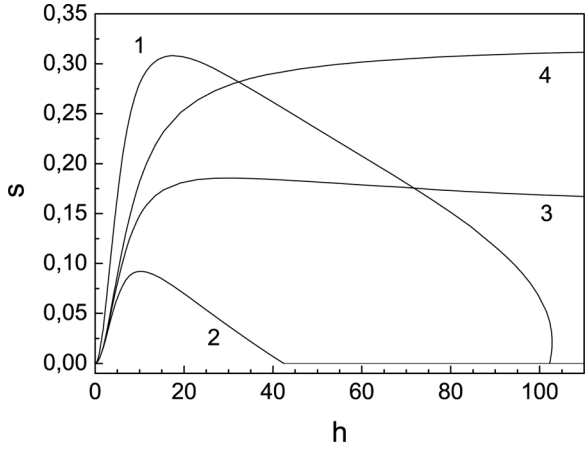

FIGURE 3 Behavior of the segregation order parameter as a function of dimensionless external field in the three ferronematic coupling regimes. Weak coupling regime: (1) $w = 4.5$, $t = 1.78 < t_c = 1.87$; (2) $w = 4$, $t > t_c = 1.32$. (3) Intermediate coupling regime: $w = 5.5$. (4) Strong coupling regime: $w = 7$. $t = 3.85$ in curves 2–4.

the continuous transition at $h = h_c(w)$ becomes first order. From Eq. (12) we find that this occurs when

$$t_c(w) \approx \frac{w_c}{2}\left(\frac{w}{w_c}\right)^3. \tag{13}$$

Substituting Eq. (11) into Eq. (10) and expanding s in powers of $(h_c(w) - h)$, we find the segregation order parameter

$$s = \frac{2w_c t_c(w)}{h_c^2(w)(t - t_c(w))}(h_c(w) - h) \tag{14}$$

in the lowest order approximation. Likewise, from Eqs. (10), (11) we find

$$\gamma_0^2 = \frac{16w^3 t}{h_c(w)(h_c^3(w) - 2w^3)(t - t_c(w))}(h_c(w) - h). \tag{15}$$

It is easy to see that there are two qualitatively different solutions separated by a singularity at $t = t_c(w)$, with $w < w_c$. For $t > t_c(w)$ we have an inverse Frederiks transition described above. For $t < t_c(w)$, the functional dependences of s, θ and ψ develop a van der Waals loop. These cases are illustrated in Figure 2 (curves 2) and Figure 3 (curve 1),

where all curves are obtained by numerical solving Eqs. (4)–(6). Dashed lines correspond to the physically unstable states of a ferronematic. To complete the picture we also show in Figure 3 the behavior of the segregation order parameter in the intermediate and strong coupling regimes.

A direct consequence of the magnetic-field induced nematic director reorientation is the birefringence of a ferronematic sample [2,4]. In contrast to the classical diamagnetic Frederiks transition this effect is nonthreshold and can be observed in a low magnetic fields <50 Oe. The potentially useful feature here is that in the presence of the inverse Fredericks effect, there will be optical bistability for $t < t_c$. This is illustrated in Figure 4, where the range of bistability is $h_c < h < 10.9 (h_c = 9.5)$ or $47.4 < H < 54.6$ Oe. Therefore, a ferronematic liquid crystal cell can act as an optical light control device or an optical shutter by the application of an alternating field when viewed between polarizers.

The optical phase lag δ is calculated using the expression:

$$\delta = \frac{2\pi D}{\lambda} \int_0^1 [n(z) - n_e] dz, \tag{16}$$

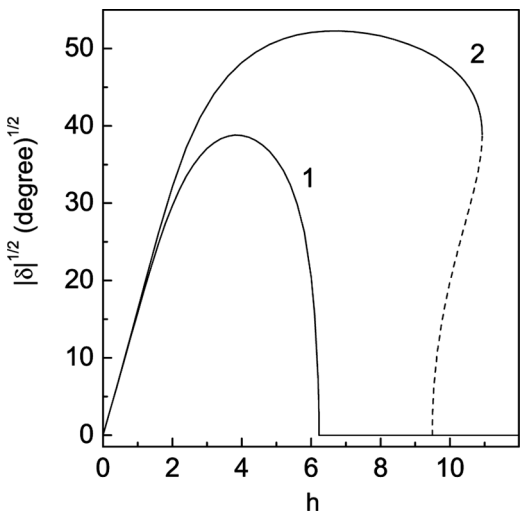

FIGURE 4 Optical phase difference for weak ferronematic coupling at finite temperature $t = 0.2$ as a function of external field. $w = 1.91$, $t > t_c = 0.15$ (curve 1) and $w = 2.42$, $t < t_c = 0.3$ (curve 2). $\lambda = 0.6328\,\mu$m, $n_o = 1.5309$, $n_e = 1.7063$.

where λ is the wavelength of the normally incident on the cell plane light,

$$n^{-2}(z) = n_o^{-2} \sin^2 \theta(z) + n_e^{-2} \cos^2 \theta(z),$$

n_e and n_o are the extraordinary and ordinary indices of refraction of the nematic. We note [2,4] that in very weak fields function $\delta^{1/2}$ is linear in the field and its slope is proportional to the volume particle fraction in the liquid crystal matrix (or the sample magnetization).

4. DISCUSSION AND CONCLUSIONS

We have analyzed in detail the behavior of a homogeneous planar anchoring ferronematic system within the weak ferronematic coupling regime at high dimensionless temperatures ($t \geq 1$) using asymptotic analysis. Experiments, however, are more commonly in the low temperature t weak coupling regime, for which the asymptotic analysis is more difficult. In this regime we have investigated the FN system by numerical computation.

The planar anchoring case seems a more sensible model system than the homeotropic case, because of the lack of bias field required to align the magnetic particles, and the higher likely response. We also note that the two systems are formally equivalent mathematically in the one constant approximation, but this equivalence disappears when bend and splay elastic constants are allowed to differ. An analogous inverse Frederiks effect occurs at weak coupling in both cases. We speculate that in the case of hybrid anchoring this is no longer the case.

In the low coupling regime the nematic response increases at low fields, reaches a maximum, then decreases and reaches zero for a critical field $h_c(w)$. We describe this transition is an inverse Frederiks effect.

For low t, high magnetic fields can cause of the ferroparticles to segregate. The coupling of segregation to the director distortion can drive the inverse Frederiks transition first order, causing bistable nematic director and optical response. The hysteretic effects have been interpreted as the signature of a decoupling of the nematic director and the ferroparticle orientation.

The high magnetic sensitivity of this system suggests that these results may be relevant in modeling magnetically-controlled devices for information processing and storage.

REFERENCES

[1] Brochard, F. & de Gennes, P. G. (1970). *J. Physique (France)*, *31*, 691.
[2] Chen, S.-H. & Amer, N. M. (1983). *Phys. Rev. Lett.*, *51*, 2298.
[3] Liang, B. J. & Chen, S.-H. (1989). *Phys. Rev. A*, *39*, 1441.
[4] Burylov, S. V. & Raikher, Yu. L. (1995). *Mol. Cryst. Liq. Cryst.*, *258*, 107; *ibid*, *258*, 123.
[5] Berejnov, V., Bacri, J.-C., Cabuil, V., Perzynski, R., & Raikher, Yu. (1998). *Europhys. Lett.*, *41*, 507.
[6] Buluy, O., Ouskova, E., Reznikov, Yu., Glushchenko, A., West, J., & Reshetnyak, V. (2002). *Mol. Cryst. Liq. Cryst.*, *375*, 81.
[7] Buluy, O., Ouskova, E., Reznikov, Yu., & Litvin, P. (2004). *Ukr. J. Phys.*, *49*, N12A, A48.
[8] Zadorozhnii, V. I., Vasilev, A. N., Reshetnyak, V. Yu., Thomas, K. S., & Sluckin, T. J. (2006). *Europhys. Lett.*, *73*, 408.
[9] Burylov, S. V., Zadorozhnii, V. I., Pinkevich, I. P., Reshetnyak, V.Yu., & Sluckin, T. J. (2002). *J. Magn. Magn. Mater.*, *252*, 153.
[10] Blinov, L. M. & Chigrinov, V. G. (1994). *Electrooptic Effects in Liquid Crystal Materials*, Springer: New York.
[11] Zakhlevnykh, A. N. (2004). *J. Magn. Magn. Mater.*, *269*, 238.
[12] Wang, Z. & Holm, C. (2003). *Phys. Rev. E*, *68*, 041401.
[13] Halperin, B. I., Lubensky, T. C., & Ma, S. K. (1974). *Phys. Rev. Lett.*, *32*, 292.